Interfacial Phenomena between Fluxes for Continuous Casting and Liquid Stainless Steel

Piotr R. Scheller

Krupp Thyssen Nirosta GmbH, D-47794 Krefeld, Germany

Abstract

Casting powders melt on the surface of the liquid metal forming a liquid slag layer. Samples taken during casting revealed convection flows in the flux layer and mass exchange with the liquid metal.

It is demonstrated that concentrations of certain elements are considerably higher at the phase boundary than in the bulk of the metal and slag phase. Disturbances of interfacial tension produced by mass and charge transfer evidently cause strong shearing forces which act in parallel with the phase boundary. These forces induce convection movements in the flow boundary layer.
Investigations into the phenomenology of convection flows next to the interface between two liquids have been carried out in laboratory experiments using various liquids. The results show that the movement velocity of volume elements next to the interface due to disturbances of interfacial tension depends on liquid layer thickness and additionally on liquid properties. A new dimensionless number describing this manner of convection flow and suitable for evaluation of experimental results is established. Its contribution to the total mass transfer will be shown. A dimensionless function describing the relation between convection flows in the slag layer and mass transfer is theoretically developed. Coefficients of this function for Ti-transfer into the flux layer have been determined empirically.

1. Introduction

Casting powders used in continuous casting fulfil various tasks such as preventing air contact, absorbing non-metallic inclusions from the liquid metal, preventing heat losses while still on the liquid metal surface, controlling heat transfer and providing lubrication at the gap between the strand shell and the mould wall. After the casting powder has melted it forms a layer of liquid slag on the surface of the molten pool which then continuously infiltrates the mould/strand gap. It is known that the chemical composition of the slag is changed by the absorption of non-metallic inclusions and reactions with metal [1-3]. As a result the physical and chemical properties of the slag change, which may have a negative effect on the quality of the strand surface. Optimising these properties can considerably reduce the occurrence of surface defects [4]. Stainless steel is characterised by high concentrations of Cr, Ni and Mo. In stabilised steels up to approx. 0.5% Ti is added. Mass transfer takes place between the liquid steel and the casting slag on the surface, with individual components of the steel alloy reacting in various ways with the slag.

Flow patterns in the fluid phases have a decisive effect on mass and heat transfer. In the case of reactions between the metal and the slag, the flows and the mixing in the slag phase determine the kinetics of the reactions[5]. Here a distinction can be drawn between large-area thermal convection flows taking place under specific conditions, and convection flows in the vicinity of the interface occurring for example in the course of chemical reactions at the phase boundary[6].
The objective of the present study was to conduct basic investigations into convection flows near the interface in laboratory studies on various model fluids and to show, based on production samples, how the mass transfer between metal and slag is affected by this manner of convection flows in the slag layer.

2. Analysis of the problem and its basic description

Convection flows
For the problem of interest here of how local disruption of the interfacial tension affects the flows in a slag layer on top of the liquid metal, first of all the conditions prevailing in a liquid layer lying on top of another without undergoing mixture are considered. From the top it is bounded by an immovable boundary, **Fig. 1**.
If the interface between two liquids is disturbed locally by the action of for example tensides or high mass transfer densities due to shifts between the phases or diffusion, the interfacial tension as a rule decreases and the adjacent liquid films on either side are pulled with the shear stress

$$t_s = \frac{\Delta\sigma}{\Delta x} \quad (1)$$

towards the not yet disrupted interface. Δs is the difference between the interfacial tension at the point of disruption and in the undisturbed area and Δx the distance between the point of disruption and the area of undisrupted interfacial tension spreading outwards in a circular manner. In fluids obeying Newton's law (e.g. the model liquids and slags used here) the shear stress given constant viscosity of the fluid is inversely proportional to the distance y from the moved surface:

$$t_v = -h\frac{dv}{dy} \approx -h\frac{\Delta v}{\Delta y} \quad . \quad (2)$$

This means that in fluid layers of different thickness between a moving (interface to water or metal) and an unmoving boundary plane (interface to glass plate – see experiment description – or sintered slag layer) for constant viscosity of the fluid with identical shear stress in the moving layer different gradients dv/dy are obtained, as shown schematically in Fig. 1. If we consider the maximum shear stress at the interface (oil/water or slag/metal), then

$$t_{max} = \frac{\Delta s}{\Delta x} = -h\frac{\Delta v}{\Delta y} \quad (3)$$

where Δv is the velocity difference between the fixed (glass plate or sintered slag layer) and the moving (water or metal) plane and Δy is the total layer thickness (oil or slag). Therefore at constant distance from the moving interface (dotted line in Fig. 1) the flow velocity and hence the impulse decreases with decreasing layer thickness.
In areas where the interfacial film breaks a new interface forms with a lower interfacial tension. Through flows and diffusion in both fluids the layers in the vicinity of the interface renew after some time with the result that the interfacial tension rises again.

To describe the flow caused by the disruption of the interfacial tension let us first consider a very thin (in extreme case monomolecular) interfacial film which between the areas of high and low interfacial tension moves away without friction from the point of disruption. The distance x from the disruption point, growing with time t, becomes the greater, the greater is the initial shear stress τ_{max} or the difference in interfacial tension $\Delta\sigma$ given otherwise constant fluid properties. This movement of the near-interface layer was observed in experiments using various fluids.

In the following, based on the similarity theory a functional relationship will be derived between a geometric parameter and the material properties in question which will make it possible to quantify the flow conditions in the vicinity of the phase boundary and to compare different material systems with each other in a dimensionless system.
The movement of a briefly accelerated volume element or fluid layer is determined by a given surface tension force F_σ (corresponding to $\Delta\sigma$) acting as a result of the disturbance in a local area on the interface, the inertia force F_ρ and the viscous force F_η. As the velocity in metallurgical systems cannot normally be measured in experiments at such short distances (movement at the boundary layer) and even in laboratory trials it is highly problematic, only the variables describing the acting forces and the characteristic length can be considered for a description of the problem (variables L_c, σ, ρ, η).
An analysis of the problem with the aid of the similarity theory gives the following number:

$$L_c \sigma \rho \eta^{-2} \equiv \frac{F_\sigma \cdot F_\rho}{F_\eta^{\,2}} \quad .$$

(4)
It describes fluid movement in the boundary layer area. An identical expression is obtained by division of the known numbers Re and We, Re^2/We.

By linking the acting forces in the form of the above-mentioned value (equation 4), the overall relationship for convection flows is maintained without flow velocity being a factor.

A reduction in the interfacial tension $\Delta\sigma$ results at the place of constant movement velocity of the volume element (in the experiment: colour marking) in decreasing amounts of shear stress $\tau = \Delta\sigma/\Delta x = -\eta\Delta v/\Delta y$ with increasing thickness of the upper liquid layer. Considered differently, at constant disruption of the interfacial tension ($\tau_{max} = \Delta\sigma/\Delta x$ = const.) with increasing thickness a constantly strong impulse is obtained at an even greater distance from the disruption.
Viewed perpendicular to the phase boundary, layers further away from the interface are also moved due to friction, with the distance covered decreasing as the impulse decreases with the distance from the interface. As stated previously, this gradient is the greater, the thinner the layer. For the respective fluid, however, τ decreases with increasing $L_c\sigma\rho\eta^{-2}$ number (because ~ L_c or Δy). It is therefore logical to use the $L_c\sigma\rho\eta^{-2}$ number to characterize the flow conditions in thin fluid layers.

Mass transfer
In considering the mass transfer between metal and slag, the following resistances are usually defined: phase boundary reaction and transfer through diffusion and convection; the greatest resistance determines the kinetics of the total mass transfer. Frequently, mass transfer is described by the Sh number, but in investigating the influence of convection flows on mass

transfer it is correct for formal reasons and experimental measurement possibilities to define the parameter characterising mass transfer according to the Bodenstein number.
To describe the results of the experiments, a modified Bodenstein number Bo* is defined which describes the ratio of the mass flux density of the species i as derived from the total mass transferred in the reaction time (measurable by sampling), to the mass flux density as derived from the diffusion velocity of the respective species from the interface through the slag layer:

$$Bo^* = \frac{\dot{m}_{i,\Sigma}}{\dot{m}_{i,D}} \quad . \tag{5}$$

$\dot{m}_{i,\Sigma}$ is calculated from the casting powder consumption and dwell time of the flux on the meniscus, and $\dot{m}_{i,D}$ using the coefficient of diffusion for the mass i .
Using the values obtainable in experiments, this definition of mass fluxes provides the following expression for the modified Bodenstein number:

$$Bo^* = \frac{L_s}{D} \cdot \frac{\dot{m}_s}{A\,\rho_s} \cdot \left(\frac{\Delta C_{i,\Sigma}}{\Delta C_{i,D}} \right) \tag{6}$$

where $\dot{m}_s$ is the melting rate of casting powder and A the reaction area equal to the cross-section of the mould.
Therefore in a fluid layer of given thickness and given physical properties, the disturbance of the force balance causes convection flows and has the following effect after the phase boundary reaction has taken place:

$$\Delta T \rightarrow v \rightarrow \dot{m} \rightarrow \Delta C \qquad \text{(thermal convection)} \tag{7}$$

$$\Delta\sigma \rightarrow v \rightarrow \dot{m} \rightarrow \Delta C \qquad \text{(interface convection)} \quad . \tag{8}$$

The driving forces ΔT (temperature difference at the lower and the upper liquid boundary) or $\Delta\sigma$ lead in this case directly to a change in the chemical composition ΔC in the reacting phase:

$$\Delta C = f(\Delta T, \Delta s) \; . \tag{9}$$

The influence of thermal convection in the flux layer on mass transfer was described in an earlier study[6].

Conclusion for interphase mass exchange
The phase boundary reactions in metallurgical processes take place very quickly[7,8]. In general it is therefore assumed that in reactions between the phases the kinetics of the overall reaction is in most cases determined by mass transfer. In the present study therefore, after a detailed investigation of the phenomenology of near-boundary flows the relationship between mass transfer in the case of slag/metal reaction and the near-boundary flows in the slag layer is investigated.
Flow and mass transfer phenomena are usually described with good approximation by empirical exponential functions. To describe the phenomena investigated here a dimensionless function was also postulated:

$$Bo^* = \text{const.} \; (L_c \sigma \rho \eta^{-2})^z \quad . \tag{10}$$

3. Experimental

Investigations into near-boundary flows

In these investigations two non-miscible fluids of different density were layered above one another. The lower fluid was distilled water and the upper oil or petroleum in various layer thicknesses. The physical properties are set out in **Table 1**. The numerical values of the $L_c\sigma\rho\eta^{-2}$ number for oil and petroleum in contact with water are lower than and higher than, respectively, the value for slag in contact with liquid metal; for example at L_c = 5 mm and assuming change of σ down to zero the values are 12 (oil), $60\cdot10^3$ (petroleum) and $2.7\cdot10^3$ to $5.4\cdot10^3$ (slag) respectively.

The influence of a local disruption of the interfacial tension on convection in the upper fluid layer was investigated in a model. The test set-up is shown in **Fig. 2**. The temperatures of the two fluids were kept equal and constant to avoid the occurrence of thermal convection flows. The fixed upper boundary between the liquid slag and the sintered layer was simulated by means of a glass plate. Highly concentrated tensides were injected into the water just below the interface. The spreading of a colour marking positioned in the upper layer directly above the interface was observed from above through the glass plate and recorded with a video camera. The tests were repeated with various thicknesses of the oil/petroleum layer after their change and cleaning of the container.

Industrial trials

The chemical composition of the steels used is shown in **Table 2**. Stainless steels with various additions of Ti were used. The chemical composition of the casting powders used is shown in **Table 3**. The data on casting powders take into consideration the C, CO_2 and moisture losses. The information on the individual compounds and elements is taken from the chemical analysis and is not indicative of the mineralogical composition of the powders and slags. The designations for molecular composition of the oxides used in this study should be viewed as being representative of all other oxidation stages unless express reference is made to specific oxidation stages. The performance of tests and sampling in the continuous casting mould has been described previously[6,12-14].

4. Results of experimental trials

Investigations into convection flows next to interface

The spreading velocity of the colour marking in the oil and petroleum layers at the phase boundary to the water was determined from video recordings. It decreases with increasing distance from the point of injection, **Fig. 3a)**. The area nearest to the injection point in which the near-interface undergoes acceleration started from a static position could not be measured for lack of a high-speed camera. The general progression of velocity as a function of distance from the injection point is sketched in **Fig. 3b)**. At constant distance from this point the movement velocity of the colour marking increases with increasing layer thickness assuming a reduction in the interfacial tension Δs by 0.018 N/m for oil and by 0.048 N/m for petroleum and constant material values. The inverse relationship for the petroleum layer of 3mm and 4mm at higher distance from the injection point is caused by generation of a circulatory flow pattern after high initial acceleration which leads to a mixing effect in perpendicular direction. The acceleration and movement velocity at similar layer thickness is much higher in the petroleum layer than in the oil layer, a result of the higher values of the $L_c\sigma\rho\eta^{-2}$ number. This means that the established number reflects the effect of the forces in the vicinity of the phase boundary with regard to flow movement. The values of the $L_c\sigma\rho\eta^{-2}$ number (compare

chapter 3) indicate that near-boundary flows in liquid casting slags should be similar to those in the petroleum layer.

Conditions at the slag/metal phase boundary
The interface between the metal and slag exhibits large and small irregularities. Large irregularities are the result of deformation of the metal surface and possible vibrations during solidification of the sample. Small irregularities with depressions, as shown in **Fig. 4a)**, are probably caused by movements at the phase boundary as a result of local fluctuations in surface tension. Similar movements can also push drops of slag into the metal, **Fig. 4b)**.

On the basis of the results shown it can be assumed that besides large-area flows[6)] boundary layer flows are also present in the slag layer.

In further investigations the concentration of some elements as a function of distance from the phase boundary in the slag and metal was measured. By removing the respective surface layer by layer the concentration profiles could be measured by Secondary Neutral Mass Spectroscopy down to a depth of around 7 :m in the metal and around 3.5 :m in the slag. The concentration profile of certain elements is discussed in the following on the basis of a sample taken during the casting of AISI 316Ti.
The concentration profile of some elements on the metal side is shown in **Fig. 5a)**. Starting from the bulk of the sample the oxygen concentration increases up to 5% to 10% at the phase boundary. A qualitatively similar progression is shown by Al, which is reduced from the slag. Cr, Mn and Ti, by contrast, are subject to strong depletion at the phase boundary, indicating their oxidation and transfer into the slag. On the slag side, **Fig. 5b)**, the oxygen concentration decreases towards the phase boundary and thus corresponds with the oxygen increase at the interface in the metal phase. A similar curve is shown by Al. The Cr oxidation is reflected in a very high concentration at the phase boundary which decreases exponentially towards the bulk of the phase. The Ti and Mn concentrations are not uniform but indicate a high amount of pick-up. The Na concentrations deserve particular mention: at the phase boundary the Na concentration increases to values of 20% to 30% with an Na_2O concentration of around 8% in the slag.
The measured concentration profiles show that on both sides of the phase boundary layers with high concentration gradients are present. The thickness of these layers is approx. 150 nm on the metal side and approx. 400 nm on the slag side. The large concentration changes at either side of the phase boundary compared with the bulk of the phases indicate that phase boundary reactions take place quickly and the kinetic of the total mass transfer is therefore determined by the transport in the phase with lower convection movement and lower diffusion velocities. As the mass transfer through the phase boundary is linked with a reduction in interfacial tension it is to be expected that the resultant interfacial convection increases the mass transfer.

Change in the mean chemical composition
The main components of the casting powders are CaO and SiO_2, which together make up approx. 60% of the mass. The physical properties of casting slags of importance to continuous casting such as viscosity and surface tension are adjusted by adding CaF_2, Na_2O, K_2O, Li_2O and FeO, MnO and MgO. Even small additions and changes in composition can have a considerable effect on these properties.

In the case of casting slag oxygen is supplied to the liquid metal from (FeO) and (SiO_2), with [Ti], [Mn] and [Cr] being oxidised. The greatest exchange, in particular with Ti alloyed steel

grades, takes place between (SiO_2) and [Ti]. Since [Ti] was present in different concentrations in the alloys examined and the change in the (TiO_2) concentration in the casting slag was the highest of all components, the effect of the convection flows on the kinetics of the metal/slag reaction was examined on the basis of its oxidation and absorption in the slag. To investigate the effect of interfacial convection flows on the kinetic of the mass transfer with liquid metal the ratio $\Delta(TiO_2)$ / [Ti] as a function of the slag layer thickness has been plotted, **Fig. 6a)** to **6c)**. Δ marks the difference in the chemical composition of sampled slag and the origin powder. This quotient increases up to slag layer thickness of 5 to 6 mm. It remains largely constant with greater slag thickness when free convection takes place which considerably improves mass transport in the slag layer[6]; as a result the equilibrium distribution value for the respective slag/metal alloy combination can be achieved shortly after the casting powder melts. With increasing casting powder consumption, from 0.40 kg/t to 0.65 kg/t to 0.70 kg/t in casting steels AISI 304, 321/316Ti and 409/430Ti, the $\Delta(TiO_2)$ / [Ti] ratio decreases. A similar change in the equilibrium distribution value with casting powder consumption was observed for the absorption of MnO in the casting slag in the casting of unalloyed steels[15]. The scattering in the results is mainly related to the difficulties in the exact estimation of the slag layer thickness and furthermore to the non uniform effect of phase boundary convection on mass transfer.

In the following the relationship between the Bo* number and the convection conditions in the slag, as defined by the $L_c\sigma\rho\eta^{-2}$ number, are examined. To analyse the problem a combination of the metal alloy and the slag is considered in each case. This ensures that the mass transfer (and thus the mass transfer coefficient) for each system considered can be seen as constant and therefore the modified Bodenstein number Bo* defined in equation (6) takes into consideration the effect of the convection conditions for each combination of slag/metal in the same way.
With $Ra < Ra_{crit}$ (Ra_{crit} =1708 is related to the conditions where the value of the $L_c\sigma\rho\eta^{-2}$ number is ca. $5\cdot10^3$) and therefore slag layer thickness < approx. 6 mm under casting conditions no thermal convection takes place and mass transfer is determined by diffusion and by phase boundary flows. In this case the equilibrium between slag and metal is not achieved in contrast to the conditions at higher slag layer thickness[6]. The $L_c\sigma\rho\eta^{-2}$ number was calculated with $\rho_S = 2.6 \cdot 10^3$ kg/m³, $\nu = 2 \cdot 10^{-5}$ m²/s and $L_c = L_S$. σ in the equation (4) was assumed as $\Delta\sigma$ (local change of interfacial tension during reaction between slag and metal) with the value of 1 N/m. To examine the relation of the mass fluxes $\dot{m}_{i,\Sigma}$/ $\dot{m}_{i,D}$ as defined by eqs. (5) and (6) the analysed concentration change in the slag $\Delta C_{i,\Sigma}$ and calculated using coefficient of diffusion $\Delta C_{i,D}$ are used. As no values are available in the literature, for D_{TiO2} a value of $5 \cdot 10^{-9}$ m²/s, i.e. 1/10 of the value for $D_{FeO} = 5.6 \cdot 10^{-8}$ m²/s[16] is assumed in the calculation of the Bo*-number. This corresponds with the value estimated by Xie and Oeters[17] on the basis of figures given in the literature for other slags of $D_{SiO2} = 5.6\cdot10^{-9}$ m²/s and should therefore represent the maximum value in relation to SiO_2. The experimental results evaluated in this way are plotted in **Figs 7a)** to **c)**. It can be clearly seen that the Bo*-number increases with increasing $L_c\sigma\rho\eta^{-2}$ number. As even with the smallest measured slag layer thicknesses the Bo* number is greater than 1 (i.e. the total mass transfer is greater than the diffusive mass transfer), it can be reliably assumed that under the experimental conditions used interfacial flows always occur as soon as liquid slag is formed. At higher values of $L_c\sigma\rho\eta^{-2}$ number than ca. $5\cdot10^3$ (marked with thick stroke) the thermal convection occurs and the relation between the Bo* number and convection flows have to be described using another function as reported previously[6]. Experimental results plotted in this range show a slightly different slope compared to the results in the range reported here.

With respect to the dimensionless function as defined by eq. (10) the relationship between mass transfer and the flow conditions in the boundary layer can be described by the following regression equations:

$Bo^* = 7.8 \cdot 10^{-5} (L_c \sigma \rho \eta^{-2})^{1.44}$ for 18-9 CrNi steel (AISI 304) (11)

$Bo^* = 1.2 \cdot 10^{-3} (L_c \sigma \rho \eta^{-2})^{1.16}$ for Ti alloyed 18-9 CrNi steel (AISI 321 and 316Ti), (12)

$Bo^* = 0.47 \cdot 10^{-3} (L_c \sigma \rho \eta^{-2})^{1.31}$ for Ti alloyed Cr steels (AISI 409 and 430Ti) . (13)

Bo* numbers for slags in contact with CrNi steels of the same basic composition but different Ti contents take on different values. With the same $L_c \sigma \rho \eta^{-2}$ number they are higher when the slag is in contact with CrNi steel alloyed with approx. 0.3% Ti (AISI 321 and 316Ti) or 0.3% to 0.5% Ti at ferritic steels (AISI 409 and 430Ti; with respect to the higher liquidus and casting temperature at this steel grades) than when it is in contact with a steel containing 0.01% Ti (AISI 304). This may be caused by the change in diffusion conditions, the change in the development of the phase boundary reaction and the change of the ionic valence which possibly influence the physical properties of the slag (viscosity).

5. Conclusions

Flow conditions due to disturbance of interfacial tension have been described theoretically and investigated experimentally. Furthermore relationships between convection flows in boundary liquid layers of continuous casting slags and mass transfer between metal and slag were examined. To this end samples were taken from the mould under operating conditions. The steels examined were CrNi and Cr steels.

The results can be summarised as follows:

1. A new dimensionless number, $L_c \sigma \rho \eta^{-2}$, describing convection flows next to the interface in the liquid boundary layer due to disturbance of interfacial tension have been established and experimentally tested.
2. With increasing values of the $L_c \sigma \rho \eta^{-2}$ number the movement velocity of the volume elements near the interface increases.
3. Phase boundary convection always occurs under continuous casting conditions regardless of the thickness of the liquid slag layer and regardless of the occurrence of free convection.
4. A dimensionless empirical function describing the relation between convection flows in the boundary slag layer and mass transfer is developed and its coefficients for Ti-transfer into the flux layer have been determined.

List of symbols

A	reaction area
Bo	Bodenstein number
Bo*	modified Bodenstein number
C	concentration
D	coefficient of diffusion
F_η	viscous force
F_ρ	inertia force
F_σ	surface tension force
L_c	characteristic length
L_S	slag layer thickness
$\dot{m}$	mass flux density
Ra	Rayleigh-number
Re	Reynold-number
Sh	Sherwood-number
T	absolute temperature
v	velocity
We	Weber-number
η	dynamic viscosity
ν	kinematic viscosity
ρ	density
σ	interfacial tension
t	shear stress
[ ]	metal phase
( )	slag phase

Indices

D	diffusion
M	metal
S	slag
Σ	total
i	substance i

References

1) Apelian, D. ; McCauley, W.L.
Iron & Steelmaker, 11(1990) 28-35

2) Emi, T. ; Nakato, H. ; Iida, Y. ; Emoto, K. ; Tachibana, R. ; Imai, T. ; Bada, H.
Proc. 61st NOH-BOS Conf. ISS-AIME Chicago, April 16-20, 1978

3) Mills, N.T. ; Bhat, B.N.
I&SM, (1978) 18-24

4) Bommarayu, R. ; Jackson, T. ; Lucas, J. ; Skoczylas, G. ; Clark, B.
I&SM (1992) 21-27

5) Steinmetz, E.
Arch. Eisenhüttenwes. 43(1972) 151-158

6) Scheller, P.R.
3rd European Conf. Cont. Casting Proc., Madrid, Spain, Oct. 20-23, 1998, pp. 797-806

7) Prange, R.
Elektochemische Untersuchungen zur Kinetik von Metall /Schlacke-Reaktionen,
Dr.-Ing. Diss., Technische Universität Clausthal, 1981

8) Prange, R. ; Heusler, K. ; Schwerdtfeger, K.
Met. Trans. 15B (1984) 281-288

9) D'Ans; Lax
Taschenbuch für Chemiker und Physiker
4. Auflage, Bd. 1
Springer Verlag Berlin, Heidelberg, New York, 1992

10) Zerbe, C.
Mineralöle und verwandte Produkte
Springer Verlag Berlin, Göttingen, Heidelberg, 1952

11) Slag atlas

2nd Edition VDEh, Verlag Stahleisen GmbH Düsseldorf, 1995
12) Hasselström, P.
Jernkontorets Forskning, IM 1468, Swedish Inst. Met. Res., Stockholm (1981)
13) Scheller, P.R.; Papaiacovou, P.
Investigations on powder behavoiur on the cc-slab caster for Cr- and CrNi-steels, in: Final Report ECSC Contract Nr. 7210-CA /160, 1995
14) Riboud, P.V.; Gatellier, Ch.; Gaye, H.; Pontoire, J.-N.; Rocabois, Ph.
ISIJ Int. 36 (1996) S22-S25
15) Chaubal, P.
Proc. 5th Int. Conf. Molten Slags, Fluxes and Salts ´97, Jan. 5-8, 1997, Sydney, Australia, pp.809-815.
16) Gmelin, L.; Durrer, R.
Metallurgie des Eisens, Bd. 5, Springer Verlag, 1978
17) Xie, H.; Oeters, F.
steel research 66 (1995) 12, 501-508

Fluid combination upper fluid lower fluid	Temp. °C	Density ρ kg m^{-3}	Viscosity η kg m^{-1} s^{-1}	Interfacial tension σ N m^{-1}	Reference
Oil Water	20	913	$84 \cdot 10^{-3}$	0.018	9, 10
Petroleum Water	20	847	$1.89 \cdot 10^{-3}$	0.048	9, 10
Liquid slag Liquid stainless steel	1460	2600	$54 \cdot 10^{-3}$ *	0.6-1.2	11

* extrapolated from own measurement up to 1330 °C

Table 1 Material data of upper liquids

Steel grade AISI No.	Liq. Temp. °C	Steel group	Chemical composition, mass % (average value)								
			C	Si	Mn	P	S	Cr	Mo	Ni	Ti
304	1456	Auste-nite	.036	.57	1.00	.023	.003	18.0	0.03	8.7	.01
321	1456		.040	.50	1.00	.023	.002	17.0	0.02	9.0	.28
316Ti	1448		.035	.50	1.00	.024	.002	16.6	2.00	10.5	.28
409	1507	Ferrite	.013	.50	0.33	.020	.002	11.5			.23
430Ti	1501		.015	.30	0.30	.020	.002	16.2			.48

Table 2 Chemical composition of tested steel grades

FeO	MnO	P	SiO_2	Al_2O_3	TiO_2	CaO	MgO	F	Na_2O	K_2O	Li_2O
1.42	0.04	0.60	34.00	8.36	0.21	36.90	0.89	8.44	8.11	0.75	1.04

Table 3 Chemical composition of used casting powder in mass %

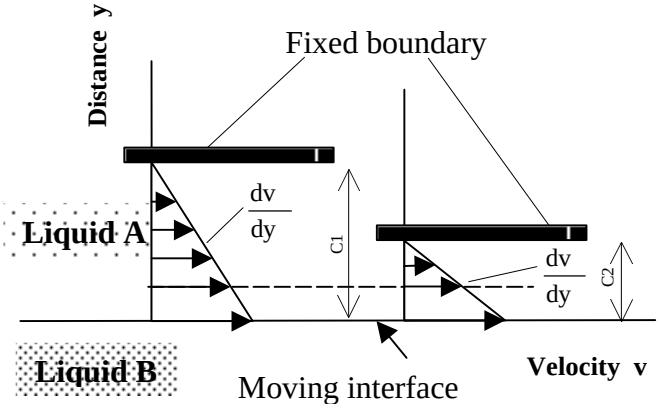

Fig. 1 Velocity vectors at different thickness of liquid layer L_c; the velocity at the moving interface is equal in both cases

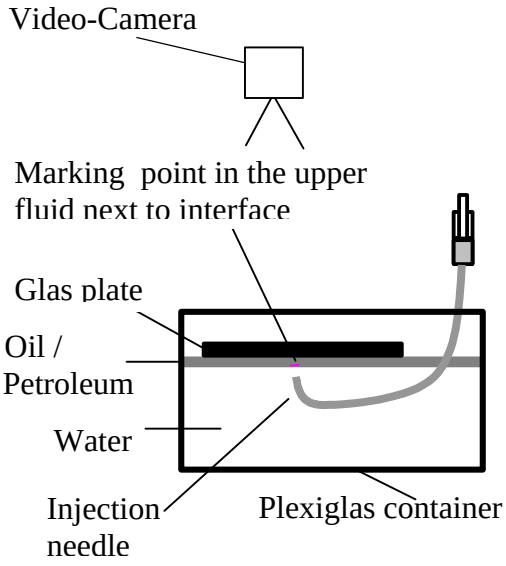

Fig. 2 Experimental arrangement for testing of interfacial convection due to disturbance of interfacial tension

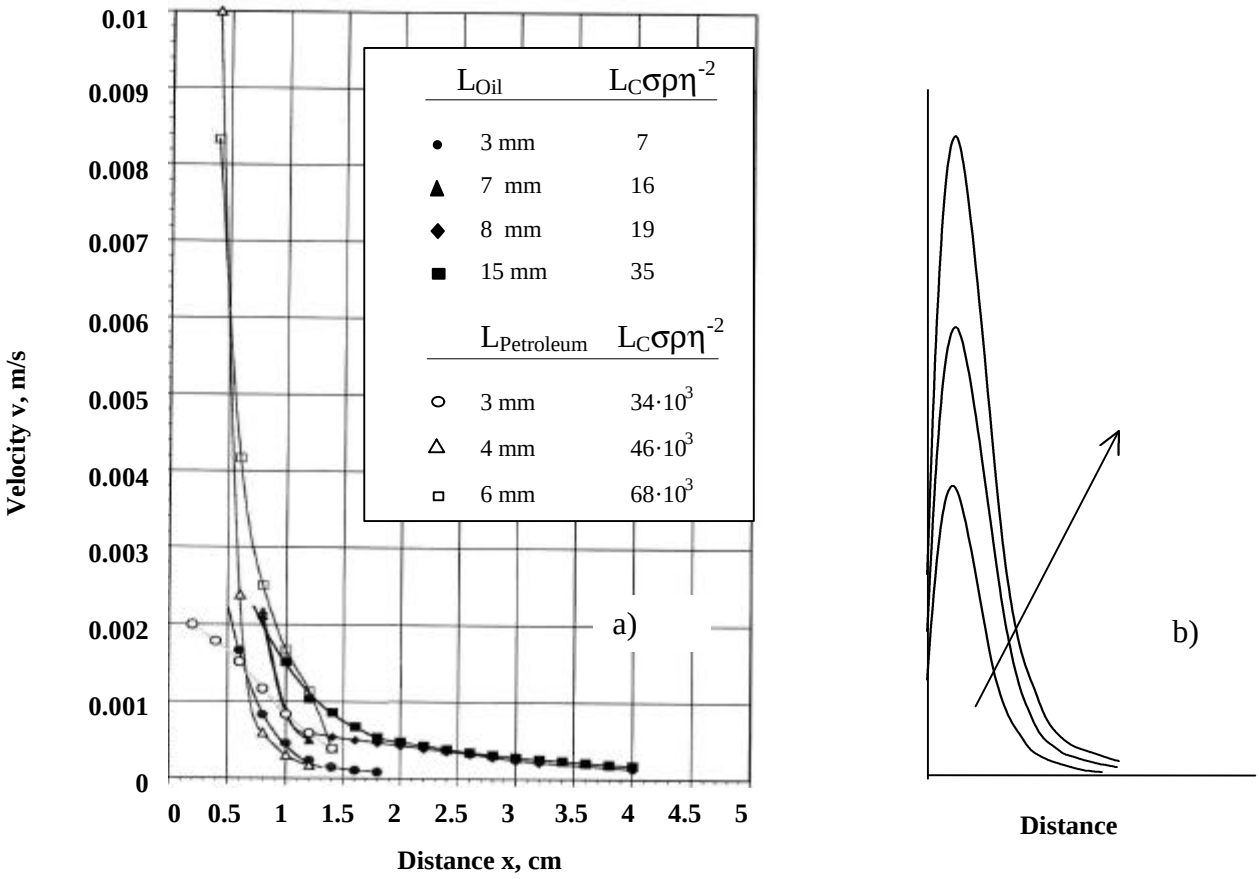

Fig. 3 Movement velocity of colour marking in the upper liquid layer set next to interface.

x = distance from the injection point (point of disturbance of interfacial tension), L = liquid layer thickness

a) Experimental results with oil/water, petroleum/water.

b) General evolution of liquid volume movement velocity as a function of the distance x. The arrow marks the evolution with increasing $L_c\sigma\rho\eta^{-2}$ –number and decreasing velocity gradient dv/dy in the layer.

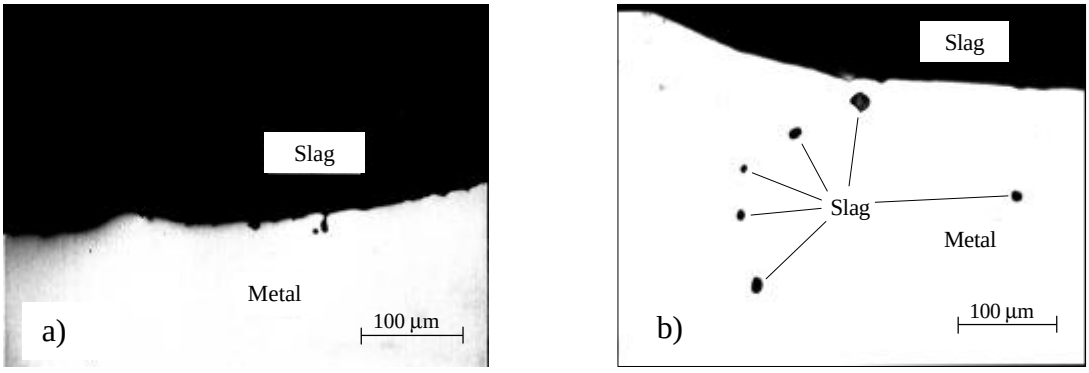

Fig. 4 Interface between metal and slag

a) Deformation of the metal-slag interface

b) Slag droplets dispersed in solidified metal

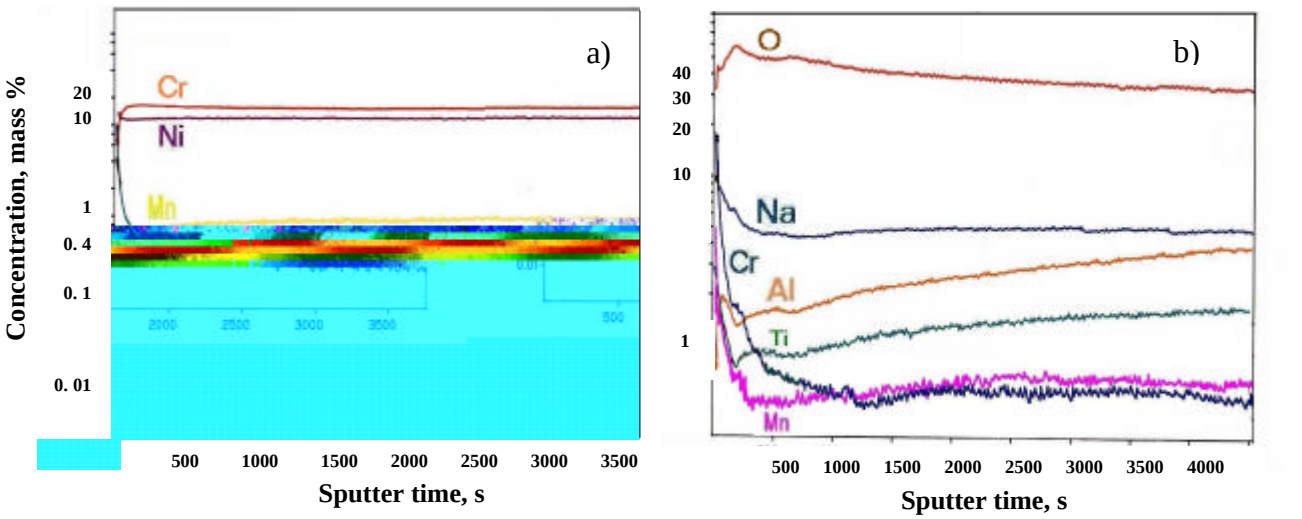

Fig. 5 Concentration of different elements as a function of the distance from the interface (cast steel: AISI 316Ti) :
a) in the metal phase (100 s sputter time = ca. 200 nm, interface at t=0 s),
b) in the slag phase (100 s sputter time = ca. 70 nm, interface at t=0 s).
Sample was taken during continuous casting operation and was quenched in water.

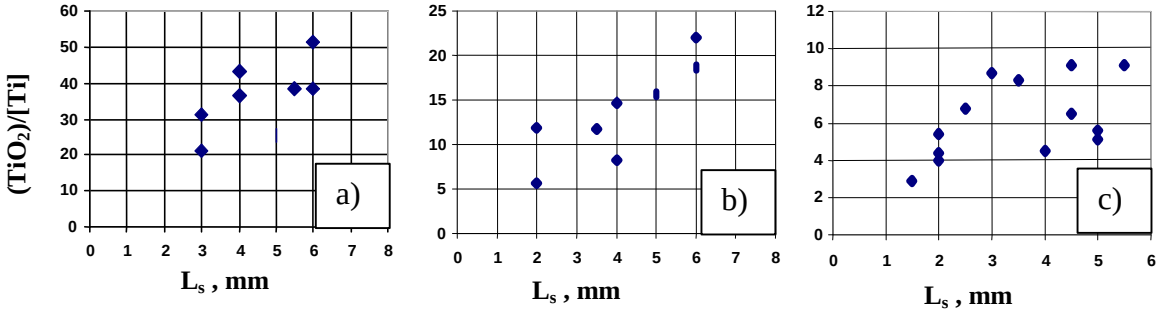

Fig. 6 The $\Delta(TiO_2)$ / [Ti]-ratio as a function of slag layer thickness; cast steel grades:
a) AISI 304 b) AISI 321 and 316Ti c) AISI 409 and 430Ti

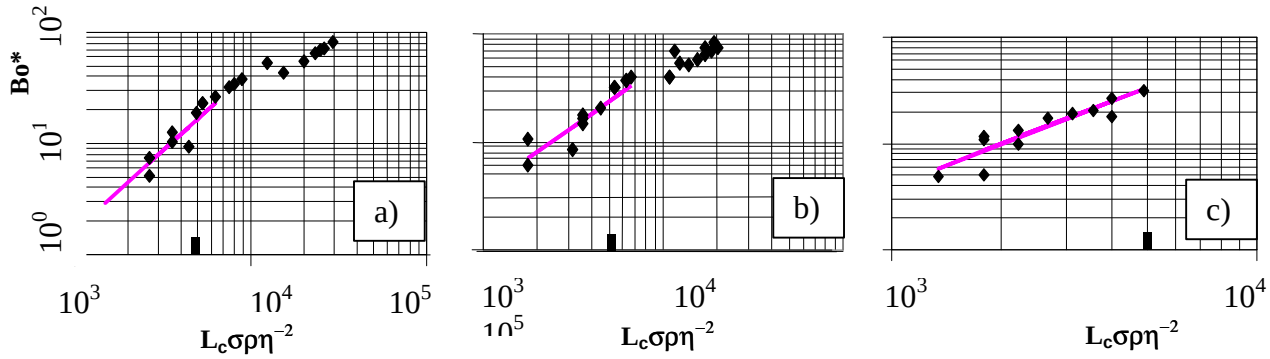

Fig. 7 Bo*-number for TiO_2-absoption into the casting flux as a function of the $L_c\sigma\rho\eta^{-2}$ number. Cast steel grades:
a) AISI 304 b) AISI 321 and 316Ti c) AISI 409 and 430Ti.